El Niño southern oscillation and its effects on world vegetable oil prices: assessing asymmetries using smooth transition models

David Ubilava and Matt Holt[†]

In this research, we examine the effects of El Niño southern oscillation (ENSO) on market dynamics of major vegetable oil prices. We adopt a smooth transition vector error correction modelling framework to analyse the impacts of ENSO events on the vegetable oil prices and, more interestingly, to investigate the asymmetric nature of the ENSO dynamics and price responses to ENSO shocks. The results confirm self-exciting type nonlinearities in the ENSO dynamics, and presence of the so-called transactions cost band in the system of vegetable oil prices. These nonlinearities yield the history-specific asymmetries in the vegetable oil price dynamics, wherein effects of ENSO shocks on the ENSO dynamics and the vegetable oil prices vary considerably between different ENSO regimes. In general, positive deviations, El Niño events, result in the vegetable oil price increase, while negative deviations, La Niña events, result in decrease in the prices. We illustrate these effects using generalised impulse-response functions and the derived asymmetry measures.

Key words: El Niño southern oscillation, smooth transition vector error correction, vegetable oil prices.

1. Introduction

Weather and agriculture are intrinsically linked. Of course, this statement is hardly controversial: crop yields in particular have long been observed to be closely tied to growing conditions. The corollary is also true: market prices for many agricultural products will necessarily be sensitive to weather shocks. There is substantial evidence of linkages between weather anomalies, agricultural production and commodity prices throughout the recorded history. For example, Temin (2002) observed that prices for barley and mustard in ancient Babylon tended to move together in a manner consistent with changing growing conditions. As well, Lamb (1995) provides evidence of extreme price spikes for cereal grains in Europe during the worst years of the Little Ice Age. And more recently, various authors have examined the role of weather events and climate change on crop yields, land prices and profitability (see Ker and McGowan 2000; Schlenker and Roberts 2006,

† David Ubilava (email: david.ubilava@sydney.edu.au) is a Lecturer at the Department of Agricultural and Resource Economics, The University of Sydney, Sydney, Australia. Matthew T. Holt is a Professor and Dwight Harrigan Faculty Endowed Fellow in Natural Resource Economics at the Department of Economics, Finance and Legal Studies, University of Alabama, Tuscaloosa, AL, USA.

2009, for examples of comprehensive empirical work on the (nonlinear) effects of weather and climate anomalies on crop yields).

Aside from the obvious connections between rainfall and temperature on crop yields, and hence prices, there is budding interest in the effects of large-scale medium-frequency climatic anomalies on various economic variables including those linked to agricultural commodity production and pricing. In part, this interest stems from a growing recognition that even local weather conditions may be linked to the medium-frequency climatic events. In recent years, attention has focussed on a particular climatic phenomenon in the Pacific Ocean. During normal conditions, equatorial trade winds blow from east to west across the tropical Pacific. However, during the so-called El Niño events, the trade winds weaken leading to a depression of the thermocline in the eastern Pacific and a corresponding elevation in the west. The result is warmer-than-normal sea surface temperatures (SSTs) in the eastern and central Pacific. These warmer SSTs in turn interact with the atmosphere, the result being that trade winds are weakened even further. Typical consequences of El Niño events are increased rainfall across the southern United States and in Peru and drought in the western Pacific region, especially in Indonesia and Australia. The counterpart to El Niño is La Niña, which is associated with intensified trade winds and colder-than-normal SSTs in the eastern equatorial Pacific. In general, La Niña episodes result in weather anomalies opposite to those for El Niños. El Niño and La Niña events usually alternate and tend to reoccur approximately every 3–7 years; the result being the so-called El Niño–La Niña cycle or the El Niño southern oscillation (ENSO). These effects were first identified in the early 1920s by Sir Gilbert Thomas Walker (Walker 1923), who eventually coined the phrase 'Southern Oscillation.'

While ENSO events take place in the tropical Pacific, they have consequences for global weather conditions and hence for agricultural commodity production and pricing. To this end, several studies have found statistically significant correlations between ENSO events and economic behaviour. In a series of papers, Paul Handler (e.g. Handler and Handler 1983; Handler 1984, 1990) provides evidence that deviations in Midwest corn yields from long-term trends are often linked to SST anomalies in the equatorial Pacific Ocean. Keppenne (1995) examined the relationship between monthly soybean futures price movements and ENSO events by using spectral analysis: a 48 month cycle in soybean futures prices related to the frequency of ENSO events was identified. The results also indicated that soybean futures were more closely linked with La Niñas, presumably due to drought conditions in the Midwest. In a related study, Letson and McCullough (2001) examined the relationship between monthly soybean cash prices and ENSO events by performing Granger causality tests; no meaningful connection between the two series was found. Finally, Debelle and Stevens (1995), Brunner (2002), and Berry and Okulicz-Kozaryn (2008) have examined the possibility that central Pacific Ocean SST anomalies affect

macroeconomic performance including measures of inflation and output. For example, Brunner (2002) has assessed linkages between ENSO events and various commodity prices along with a measure of inflation and GDP growth for G7 countries; he found that ENSO events apparently have considerable explanatory power for commodity price movements in many instances.

While several of the foregoing studies provide enticing evidence about possible relationships between ENSO events and commodity price movements, more work is required. To begin, there is mounting evidence that the ENSO cycle is not adequately described by linear dynamics, and therefore, linear time series methods may not be appropriate. For example, Hall *et al.* (2001) find evidence that the autocorrelations in ENSO anomalies are different in El Niño versus La Niña regimes. An (2009) provides a current review of research on nonlinearities in the ENSO cycle in the climatology literature and makes special note of observed El Niño–La Niña asymmetries. As well, there is mounting evidence that time series observations for many commodity prices may be more adequately characterised by nonlinear dynamic relationships. For example, Shahwan and Odening (2007) and Ahti (2009) show that nonlinear models based on artificial neural networks and smooth transition autoregressions (STAR) can yield improved commodity price forecasts relative to linear ones.

Additionally, Balagtas and Holt (2009) find evidence that a number of commodity prices behave in a manner consistent with regime-dependent nonlinearity. There are several reasons for this. First, it is due to the very nature of the production–distribution cycle: while agricultural crops are usually harvested on an annual basis, given the demand shock they can be disposed promptly, thus suggesting possibilities for asymmetric price dynamics (Holt and Craig 2006; Ubilava 2012). Second, in the system of closely related (substitute) products, an additional source of nonlinear behaviour arises due to pretense of the so-called transactions cost band: when prices are in disequilibrium, a price shock to one or several commodities will typically result in prompt and adequate adjustments by economic agents, resulting in a closer co-movement of prices; while when prices are such that they are within the transactions cost band, economic agents may be reluctant to react to small variations in one or more of the prices, thereby potentially mitigating co-movement due to the substitution effects on the related commodities (Balke and Fomby 1997).

What the foregoing discussion makes clear is that while there may be evidence of nonlinear dynamics in ENSO events and, as well, in commodity price movements, to date the two have not been considered together. That is our focus here. Specifically, in this paper, we examine the effects of ENSO events on market dynamics of world vegetable oil prices. There is evidence that ENSO events have significant impacts on the production and prices for vegetable oils, most notably for palm oil, which is produced primarily in South-East Asia (see, e.g. Brunner 2002). We also conjecture that responses to ENSO shocks are asymmetric—a strong El Niño event may result in price

dynamics for vegetable oils that are very different than those associated with a strong La Niña event. This later observation suggests that standard linear models including vector autoregression (VAR) or vector error correction models (VECMs)—models of the sort employed, for example, by In and Inder (1997) and Owen *et al.* (1997)—may not be appropriate for examining relationships between ENSO events and vegetable oil prices. As noted recently by Ismail (2011), models for related vegetable oil prices should allow for the possibility of asymmetric or nonlinear adjustments irrespective of the role of ENSO events.

A central contribution of this paper is therefore to combine all of the aforementioned features in a comprehensive modelling framework, and by so doing to report on the most thorough analysis to date of the impacts of an important climatic anomaly—ENSO—on interrelated commodity prices. Specifically, we use the STAR modelling framework of Teräsvirta (1994) to examine the potential for nonlinear dynamics in the ENSO cycle as well as within a system of vegetable oil prices. To do so a multivariate version of the STAR model—the smooth transition vector error correction model (STVECM) similar to that of Rothman *et al.* (2001)—is used to model a system of interrelated vegetable oil prices. Smooth transition framework is a generalisation of a more restricted threshold autoregressive (TAR) models of Tsay (1989); Tong (1990). Additionally, it embeds elements of other complex time series models, such as Markov switching (e.g. Hamilton 1989), and artificial neural network (e.g. Kuan and White 1994) models. An attractive feature of the STAR-type models is that they allow for a possibility of a continuum of switching points between the regimes. This could be crucial when considering behaviour of potentially heterogeneous agents, for example. Additionally, because the growing and harvesting seasons of the considered crops differ depending on the country of origin, the aforementioned nonlinearities associated with supply and distribution dynamics could be mitigated, and thus, a smooth transition between the regimes could be a more appropriate nonlinear modelling technique.

In what follows, we will first present a brief overview of the vegetable oils industry. We will then outline the modelling framework of this research, followed by the empirical analysis, where we describe data used in the research and present main findings of this study. We will illustrate the effects of various ENSO shocks by implementing generalised impulse-response functions (GIRFs).

2. Vegetable oils: a brief overview

The fats and oils industry is important in international trade, consumption and pricing and therefore has long been of interest to economists. In the literature, particular attention has been paid to substitutability amongst different oils (see, e.g. Labys 1977; In and Inder 1997; Owen *et al.* 1997; Ismail 2011). These and related studies have established that even though

vegetable oils are similar in terms of chemical composition and end-use, they are by no means perfect substitutes. Nonetheless, several subgroups of fats and oils share many of the same properties and characteristics and thus are considered to be truly close substitutes. Specifically, the most prevalent of these, both from production and consumption standpoints, is a group consisting of four major vegetable oils: palm, soybean, rapeseed and sunflowerseed (see, e.g. Schmidt and Weidema 2008). These oils constitute approximately 85 per cent of world vegetable oil production and about 90 per cent of world vegetable oil trade (see Figure 1). They also share many common end-uses including food preparation, soap production and manu-facturing of paints and medicines. Additionally, each is currently used in biodiesel production (e.g. Demirbas 2008), thereby further strengthening price linkages amongst the oils in this group. Indeed, the reasonably high degree of substitutability between palm, soybean, rapeseed and sunflowerseed oils suggests their prices are likely to co-move (In and Inder 1997).

Due to increased global demand, there has been considerable growth in the production of all major oils over the past several decades. Even so, palm oil production has increased most dramatically, and currently, it is the most produced and exported oil in the world (PSD Online 2011). Of particular interest is that over 85 per cent of palm oil is produced in two countries: Indonesia and Malaysia. Moreover, in these countries, production growth has resulted largely from the expansion of area planted to palm trees rather than from yield increases (e.g. Carter *et al.* 2007).

Unlike palm oil, production of the remaining oils is not as tightly concentrated geographically. For example, soybean oil, the second largest vegetable oil in terms of production and trade, is produced in different regions of North and South America, Europe and Asia; however, the top three soybean oil–exporting countries are the United States, Brazil, and Argentina. Likewise, rapeseed oil is produced in different parts of the world, with Canada being the largest exporter. And finally, sunflowerseed oil is
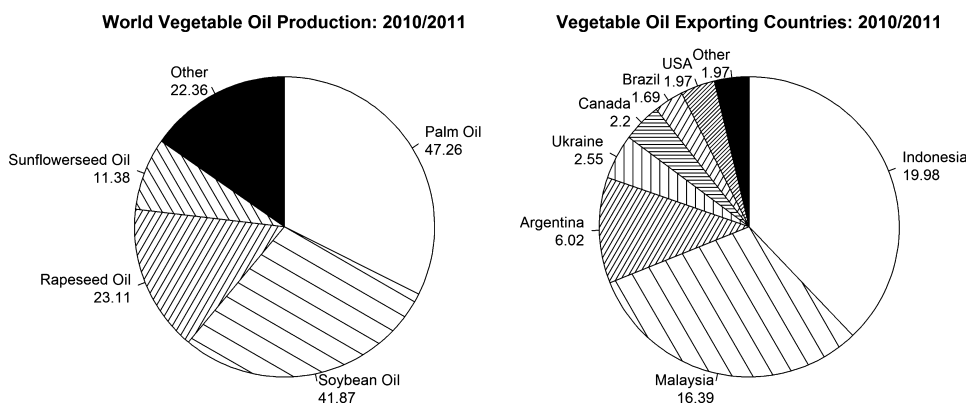
Figure 1 Major vegetable oil production and exports. Note: Values represent Million Metric Tons.

produced largely by European countries, with Ukraine being the largest exporter of this oil (PSD Online 2011).

While it is apparent that the vegetable oil production takes place in different parts of the world, it is nontrivial that production of the world's most exported (60% of total vegetable oil exports) oil, that is, palm oil, is concentrated in Indonesia and Malaysia. The implication is that extreme weather conditions in a given year will have a negative impact on palm oil production in these countries and therefore will have implications for palm oil price. As well, given that palm, soybean, rapeseed and sunflowerseed oils are apparently close substitutes in consumption, it seems likely that any such shock to palm oil production and hence price will likely have spillover effects on the prices for these other oils as well (again, see In and Inder 1997).

What, then, might underlie a palm oil production shock? Aside from changes in area (once brought into production palm trees typically produce oil for upwards of 25 years), weather conditions can have important implications for palm oil production (see, e.g. Casson 1999). In particular, extreme drought reduces yields several months or more into future. Incidentally, El Niño impacts in particular can be quite severe throughout South-East Asia, including Malaysia and Indonesia: strong El Niño events in this region are typically associated with correspondingly strong drought conditions (see, e.g. Enfield 2003). The relationship between El Niño and palm oil production in particular has also been noted in the popular press and in a series of technical reports. For example, during the most recent El Niño event, that is, from late 2009 through early 2010, a spate of articles appeared linking El Niño events to price spikes in palm oil (see for example Berthelsen 2009; Bromokusumo and Meylinah 2009).

What has received virtually no attention are the potential spillover or secondary effects that these events likely have on prices for closely related fats and oils. Earlier work by Brunner (2002) provides some tantalising evidence in this regard—he reports that El Niño events have a significant impact on palm, soybean, groundnut and coconut oils. But his results were not obtained by allowing for dynamic feedbacks amongst the various oil prices, that is, substitutability amongst prices was not considered. Moreover, and as previously noted, he assumed that the dynamics governing the evolution of ENSO were linear. We now turn to a discussion of a modelling framework that incorporates these various features.

3. The modelling framework

In this section, we outline the econometric approach used to investigate nonlinear dynamic relationships between ENSO and vegetable oil prices. We begin by reviewing standard linear modelling techniques for a single equation, followed by a discussion of STAR-type models. We then describe a general econometric framework for specifying smooth transition VECMs.

3.1. Smooth transition autoregressive models

Linear autoregressive models are the basic building block of the STAR modelling framework. An autoregressive model of order p, an $AR(p)$, in first difference form is written as

$$\Delta y_t = \phi' \mathbf{x}_t + \varepsilon_t, \tag{1}$$

where Δ is a first-difference operator; y_t is a dependent variable of interest; $\mathbf{x}_t = (1, \Delta y_{t-1}, \ldots, \Delta y_{t-p+1}, y_{t-1}, z_{1,t}, \ldots, z_{m,t})'$ is a vector of right-hand-side variables; $z_{j,t}, j = 1, \ldots, m$ are exogenous variables including seasonal indicator variables; $\phi = (\alpha, \beta_1, \ldots, \beta_{p-1}, \beta_0, \delta_1, \ldots, \delta_m)'$ is a vector of parameters to be estimated; and finally, $\varepsilon_t \sim iid(0, \sigma^2)$ is an additive error process. Note that if y_t follows a unit root process $\beta_0 = 0$; otherwise, we expect that $\beta_0 < 0$.

The linear model in (1) is easily generalised to allow for nonlinearities in a manner consistent with Teräsvirta's (1994) STAR framework. Specifically, consider

$$\Delta y_t = \phi_1' x_t [1 - G(s_t; \gamma, \mathbf{c})] + \phi_2' \mathbf{x}_t G(s_t; \gamma, \mathbf{c}) + \varepsilon_t, \tag{2}$$

or, alternatively,

$$\Delta y_t = \varphi_1' \mathbf{x}_t + \varphi_2' x_t G(s_t; \gamma, \mathbf{c}) + \varepsilon_t, \tag{3}$$

where in (3) $\varphi_1 = \phi_1$ and $\varphi_1 = \phi_2 - \phi_1$. In either case, $G(s_t; \gamma, \mathbf{c})$ is a transition function that is strictly bounded between zero and one. The transition function in turn varies with s_t, the transition variable, which is often specified to be some function of lagged values of y_t. Alternatively, s_t might be specified to be a function of time, resulting in the class of time-varying autoregressions, or TVARs, pioneered by Lin and Teräsvirta (1994). The other determinants of $G(.)$ are the parameters γ and c, where γ, the speed-of-adjustment parameter, determines how rapidly shifts from one regime to another occur and where c, a set of centrality parameters, determines the value(s) of s_t around which regime changes are centred.

There are several choices for the specification of the transition function. The most popular is the logistic function, which can be written in general form as

$$G(s_t; \gamma, \mathbf{c}) = \left[1 + \exp \left\{ -\left(\frac{\gamma}{\sigma_{s_t}^k} \right) \prod_{j=1}^{k} (s_t - c_j) \right\} \right]^{-1}, \gamma > 0, c_1 \leq \ldots \leq c_k, \tag{4}$$

and where $c = (c_1, \ldots, c_k)$ is a vector of centrality parameters. In practice, most analysts choose either $k = 1$ or $k = 2$ (Lin and Teräsvirta 1994). When $k = 1$ and when (4) is combined with (2), the resulting model is a member of the logistic STAR, or LSTAR family, and is useful in situations where asymmetry in dynamic responses to s_t exists. Likewise, when $k = 2$, the

resulting model is a member of the quadratic STAR, or QSTAR family (Jansen and Teräsvirta 1996), and is useful for situations where nonlinearity is linked to the absolute value of s_t.

The transition function may also be specified by using an exponential representation, expressed as

$$G(s_t; \gamma, c) = 1 - \exp\left\{-\left(\frac{\gamma}{\sigma_{s_t}^2}\right)(s_t - c)^2\right\}, \gamma > 0, \tag{5}$$

where parameters and variables are as defined previously. The exponential and quadratic functions have similar properties in that both are useful for modelling changing dynamics associated with the magnitude of the absolute value of the transition variable. Finally, in (4) and (5), the parameter γ is normalised by $\sigma_{s_t}^k$, where σ_{s_t} is the standard deviation of the transition variable, s_t. Doing so effectively renders γ unit free. Figure 2 illustrates hypothetical representations for the LSTAR, QSTAR and ESTAR transition functions for different values of $\mathbf{c}$ ($c = 0$ for LSTAR and ESTAR, and $\mathbf{c} = (-1, 1)$ for QSTAR) and γ, the speed-of-adjustment parameter ($\gamma = (0.5, 2, 10)$).

3.2. Smooth transition vector error correction models

The smooth transition autoregressive framework can be extended to a multivariate framework. One specific case of interest is the STVECM considered first by Rothman *et al.* (2001), and specified as follows:

$$\Delta\mathbf{x}_t = \boldsymbol{\alpha}_1\hat{\mathbf{e}}_{t-1} + \sum_{j=1}^{p-1}\Gamma_{1,j}\Delta\mathbf{x}_{t-j} + \Psi_1\mathbf{z}_t$$
$$+ \left(\boldsymbol{\alpha}_2\hat{\mathbf{e}}_{t-1} + \sum_{j=1}^{p-1}\Gamma_{2,j}\Delta\mathbf{x}_{t-j} + \Psi_2\mathbf{z}_t\right)\iota G(s_t, \gamma, \mathbf{c}) + \boldsymbol{v}_t \tag{6}$$

where $\mathbf{x}_t = (y_{1,t}, \ldots, y_{n,t})'$ is a $n \times 1$ vector of dependent variables; $\mathbf{z}_t$ is a $m \times 1$ vector of exogenous variables and/or seasonal dummies. Likewise,
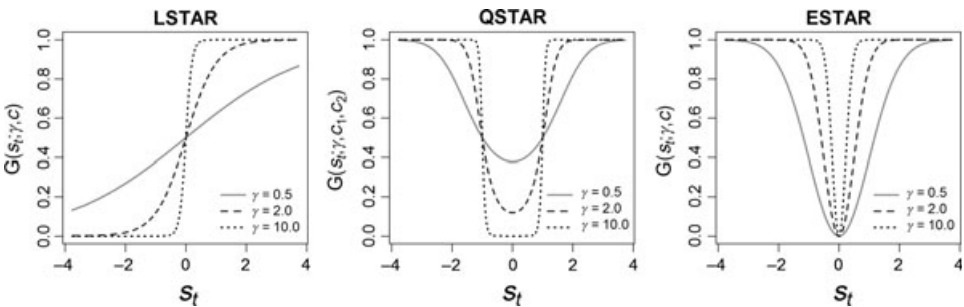
Figure 2 Representative LSTAR, QSTAR and ESTAR transition functions.

$\hat{\mathbf{e}}_{t-1} = \beta'(\mathbf{x}'_{t-1}, 1)$ is a vector of estimated error correction terms, such that $\Pi_k = \boldsymbol{\alpha}_k \boldsymbol{\beta}'$ is a matrix of parameters defining the long-term dynamics between the variables in the system, where $\boldsymbol{\beta}$ is a matrix of cointegrating vectors, such that $\boldsymbol{\beta}'\mathbf{x}_t$ is a stationary process (even though $\mathbf{x}_t$ itself is not); and $\boldsymbol{\alpha}_k$, $k = 1,2$, is a matrix of speed-of-adjustment parameters. As well, $\Gamma_{k,j}$ and Ψ_k, $k = 1,2$ and $j = 1,\dots,p-1$, are matrices (vectors) of parameters to be estimated. $\iota G(s_t, \gamma, \mathbf{c})$ is a vector of transition functions, where ι is an n-dimensional unit vector restricting the transition function to be common across the equations—a restriction that has been imposed in most prior research investigating STVECMs (see for example Rothman *et al.* 2001; Milas and Legrenzi 2006; Milas and Rothman 2008; Goodwin *et al.* 2011). Finally, $\upsilon_t \sim N(0, \Sigma_\upsilon)$, where Σ_υ is a $n \times n$ positive definite covariance matrix.

4. Data

We employ monthly data for the ENSO anomaly and for vegetable oil prices covering the period between January 1972 through December 2010. The ENSO variable is constructed as SST anomalies for the *Niño 3.4* region of the central Pacific, and is derived from an index tabulated by NOAA's Climate Prediction Center. Specifically, this index measures the difference in SSTs in the area of the Pacific Ocean between 5°N-5°S and 170°W-120°W and is thus a strong indicator of ENSO activity. As well, the monthly measure is an average of daily values interpolated from weekly measures, which in turn are obtained from both satellites and buoys. The anomaly is the deviation of the *Niño 3.4* monthly measure from the historic average for the same month for the 1971–2000 period.

Vegetable oil price data are for palm, soybean, rapeseed and sunflower-seed oils and were obtained from ISTA Mielke GmbH, better known as the Oil World. All vegetable oil prices are in U.S. dollars per tonne and are either Free on Board (FOB) or Cost, Insurance, and Freight (CIF). All prices are deflated by using the Producer Price Index for commodities, obtained from the U.S. Bureau of Labor Statistics. Further, real prices were transformed by taking natural logarithms, so that changes are expressed in percentage terms. Hereafter, any reference to a vegetable oil price implies the real price in natural logarithmic form, unless stated otherwise. Figure 3 shows a plot of vegetable oil prices over the sample period. It is clear from this figure that prices have a strong tendency to move together (co-movement).

5. Estimation

For estimation purposes, we treat ENSO as a strictly exogenous variable. That is, vegetable oil prices are contemporaneously correlated with ENSO and are affected by lagged levels of ENSO, but not the other way around.
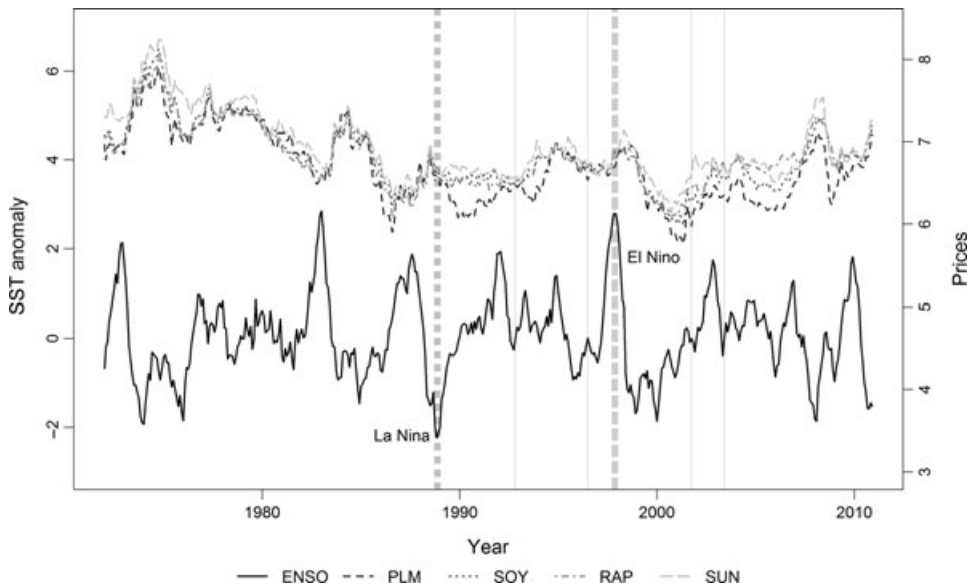
Figure 3 El Niño southern oscillation (ENSO) sea surface temperatures (SST) anomaly and major vegetable oil prices: 1972–2010. Note: SST Anomaly is expressed in $°C$; prices represent natural logarithms of the vegetable oil prices expressed in 2010 U.S. Dollars.

This assumption is hardly counterintuitive in that climatic events are unlikely to be affected by commodity prices or other economic variables, at least in the short or intermediate run. This assumption is, moreover, supported by the findings in earlier studies (e.g. Brunner 2002). Therefore, we first estimate the ENSO equation independently as a univariate process. We then estimate the system of vegetable oil price equations, where ENSO enters as an exogenous forcing variable.

5.1. The ENSO equation

We begin with a linear AR model for the ENSO series. Based on Akaike Information Criterion (AIC), a lag length of $p = 5$ was chosen. Further, unit root tests (i.e. augmented Dickey–Fuller tests) indicated that the null hypothesis of a unit root could be rejected for this series at $\alpha = 0.01$ significance level. We therefore proceed by modelling the ENSO variable as in (1), that is, with a lagged level values for the ENSO variable included as a right-hand-side variable (such a specification is preferred to a more straightforward autoregression in levels, because it allows for the possibility of a unit root in one of several regimes in a regime-dependent autoregressive set-up).

To identify regime-dependent nonlinearities, we adopt a testing framework of Luukkonen *et al.* (1988), where an auxiliary regression approach is

proposed to circumvent the nuisance parameters identification problem, also known as the Davies' problem (Davies 1977, , 1987). Two sets of transition variables were examined initially: lagged levels of ENSO, ENSO_{t-d}, where $d = 1,\ldots,12$, and, moving averages of ENSO, $\frac{1}{\bar{d}}\sum_{i=1}^{\bar{d}} \text{ENSO}_{t-i}$, where $\bar{d} = 1,\ldots,12$. Test results for the moving average transition variable are presented in Table 1. A more thorough outline of the testing procedure and a complete set of nonlinearity test results are reported in the Technical Appendix (D. Ubilava and M. Holt, unpubl. data, 2012). STAR models were then estimated by using the consecutive candidate transition variables, the one with the lowest p-value in the nonlinearity test being considered first. The final selection is made such that the estimated STAR model has an improved fit relative to the linear model, based on AIC; the two regimes are seemingly identified, and evidence of remaining nonlinearities is minimised. See the Technical Appendix (D. Ubilava and M. Holt 2012, unpubl. data, 2012) for a set of remaining nonlinearity test results. Based on these criteria, as well as the results of additional diagnostic tests (i.e. tests for no remaining parameter nonconstancy and for no remaining residual autocorrelation), we selected $\frac{1}{3}\sum_{i=1}^{3} \text{ENSO}_{t-i}$ as the most suitable transition variable. We therefore define an empirical version of the STAR model for ENSO as follows:

$$
\Delta\text{ENSO}_t = \left(\alpha_1 + \beta_1 \text{ENSO}_{t-1} + \sum_{j=1}^{4} \phi_{j,1}\Delta\text{ENSO}_{t-j} + \boldsymbol{\delta}_1' \mathbf{D}_t \right)
$$
$$
+ \left(\alpha_2 + \beta_2 \text{ENSO}_{t-1} + \sum_{j=1}^{4} \phi_{j,2}\Delta\text{ENSO}_{t-j} + \boldsymbol{\delta}_2' \mathbf{D}_t \right) G(\hat{s}_{t-3}; \gamma, c) + \varepsilon_t
$$

$$(7)$$

where D_t is a vector of monthly dummy variables; other variables and parameters are as defined in (1) and (3).

5.2. The system for vegetable oil prices

Let $\mathbf{x}_t = (P_t^{\text{PLM}}, P_t^{\text{SOY}}, P_t^{\text{RAP}}, P_t^{\text{SUN}})'$ be a vector of observations at time t for vegetable oil prices. Based on standard ADF tests, reported in the Technical Appendix (D. Ubilava and M. Holt 2012, unpubl. data, 2012), all vegetable oil prices apparently contain a unit root. However, given the close substitutability between the vegetable oils, and apparent co-movement of prices, one or more linear combinations of these prices are likely to be stationary, that is, cointegrated. In this event, the system of equations can of course be modelled in vector error correction form. Indeed, Johansen test results support the hypothesis of cointegration with two unique cointegrating vectors being identified. Details are available in the Technical Appendix (D. Ubilava and M. Holt, unpubl. data, 2012). Based on the AIC, the lag length for the endogenous variables in the system was set to four.

Table 1 Nonlinearity test results for the El Niño southern oscillation (ENSO) equation

Transition variable	H'_0	H_{04}	H_{03}	H_{02}	Model
s_{t-1}	3.00E-06	4.90E-01	8.00E-01	7.40E-11	LSTAR
s_{t-2}	8.10E-07	5.30E-01	5.50E-01	3.90E-11	LSTAR
s_{t-3}	**8.70E-08**	**4.70E-01**	**2.90E-01**	**1.20E-11**	**LSTAR**
s_{t-4}	7.10E-08	6.20E-01	2.20E-01	7.00E-12	LSTAR
s_{t-5}	2.00E-08	4.50E-01	1.90E-01	4.80E-12	LSTAR
s_{t-6}	2.30E-08	4.20E-01	1.50E-01	1.10E-11	LSTAR
s_{t-7}	2.30E-08	3.30E-01	8.10E-02	6.40E-11	LSTAR
s_{t-8}	1.80E-08	1.60E-01	4.80E-02	5.70E-10	LSTAR
s_{t-9}	6.60E-09	3.50E-02	3.10E-02	4.50E-09	LSTAR
s_{t-10}	5.30E-09	1.20E-02	2.20E-02	3.00E-08	LSTAR
s_{t-11}	1.60E-08	9.40E-03	1.80E-02	2.30E-07	LSTAR
s_{t-12}	1.60E-07	1.10E-02	2.40E-02	2.30E-06	LSTAR
F_{RN}	3.80E-01	6.80E-01	3.80E-01	1.90E-01	
F_τ	4.90E-01	9.40E-01	6.30E-01	4.60E-02	
F_{AC}	1.20E-01				

Note: the values in the table represent probability values of the hypotheses being tested; the values in bold represent the selected transition variable and the associated transition function. The column headed with H'_0 corresponds with the null hypothesis of linearity; the columns headed with H_{04} and H_{02} correspond with the embedded test against logistic nonlinearity, while the column headed with H_{03} corresponds with the test against exponential/quadratic nonlinearity; the appropriate models are presented in the column headed with Model. Further, $s_{t-d} = \frac{1}{d}\sum_{i=1}^{d} \text{ENSO}_{t-i}$, where $d = 1,\ldots,12$ and $\bar{d} = 1,\ldots,12$. Finally, F_{RN}, F_τ and F_{AC} denote tests against remaining nonlinearity (with respect to the transition variable of choice, i.e. s_{t-3}), parameter nonconstancy and residual autocorrelation, respectively.

Additionally, we incorporate the current and up to and including two lags of the ENSO variable in each equation of the system, wherein the ENSO lags also selected based on AIC. Finally, we include monthly binary variables to account for possible seasonal effects.

The next step is to test for nonlinearity in the system and, if identified, to specify a suitable transition function. We adopt a testing framework proposed by Camacho (2004) to assess potential nonlinearities in the system. See the Technical Appendix (D. Ubilava and M. Holt 2012, unpubl. data, 2012) for the details. The candidate transition variables are lags of a simple average of the two error correction terms, $\bar{\bar{e}}_{t-d}$, where $d = 1,\ldots,12$. Thus, we intend to examine nonlinearities in vegetable oil price dynamics in relation to the long-run equilibrium between the prices. The intuition is that adjustments to long-run equilibrium may occur at differing rates depending on a direction or a magnitude of the deviation from equilibrium. The nonlinearity test results are presented in Table 2. Preliminary results revealed that there is little evidence of nonlinearities in seasonal effects, although is substantial evidence of nonlinearities in the system's autoregressive components. Further, the evidence reported in Table 2 points firmly in the direction of model a transactions cost band, that is, either an exponential or a quadratic STVECM. We therefore proceed by fitting exponential and quadratic STVECMs using the candidate transition variables identified in Table 2, while restricting the parameters associated with the seasonal indicator variables to enter the system in linear form. The selection criteria are similar

to those used in the case of ENSO equation. The result is that we selected $\bar{\hat{e}}_{t-7}$ as the most suitable transition variable when combined with an exponential transition function. Based on the system AIC, the estimated STVECM improves overall model fit. The empirical version of the STVECM of the vegetable oil prices is therefore specified as

$$
\begin{aligned}
\Delta \mathbf{x}_t = & \left(\boldsymbol{\alpha}_1 \hat{\mathbf{e}}_{t-1} + \sum_{j=1}^{3} \Gamma_{j,1} \Delta \mathbf{x}_{t-j} + \Psi_1 \mathbf{ENSO} + \Psi_D \mathbf{D}_t \right) \\
& + \left(\boldsymbol{\alpha}_2 \hat{\mathbf{e}}_{t-1} + \sum_{j=1}^{3} \Gamma_{j,2} \Delta \mathbf{x}_{t-j} + \Psi_2 \mathbf{ENSO} \right) \iota G(\bar{\hat{e}}_{t-7}, \gamma, c) + \upsilon_t,
\end{aligned}
\tag{8}
$$

where $\mathbf{ENSO} = (\mathrm{ENSO}_t, \mathrm{ENSO}_{t-1}, \mathrm{ENSO}_{t-2})'$ is a vector of current and lagged values of the ENSO variable; $\mathbf{D}_t$ is a vector of monthly dummy variables; other variables and parameters are as defined in (6).

5.3. The estimated transition functions

The estimated transition functions for the ENSO forcing variable and for the system of vegetable oil prices are, respectively,

$$
\hat{G}(s_t; \hat{\gamma}, \hat{c}) = \left\{ 1 + \exp \left[-\underset{(1.036)}{2.133} \Big/ \sigma_e \left(\frac{1}{3} \sum_{i=1}^{3} \mathrm{ENSO}_{t-i} + \underset{(0.244)}{0.018} \right) \right] \right\}^{-1}
\tag{9}
$$

and

$$
\hat{G}(s_t; \hat{\gamma}, \hat{c}_1, \hat{c}_2) = 1 - \exp \left[-\underset{0.435}{(1.325)} \Big/ \sigma_s^2 \left(\bar{\hat{e}}_{t-7} + \underset{0.020}{(0.086)} \right)^2 \right]
\tag{10}
$$

where $\sigma_e = 0.895$ and $\sigma_s = 0.293$ and where values in parentheses are asymptotic standard errors. The estimated γ values in (9) and (10) imply that regime transitions in both instances should be relatively smooth and, indeed, as reported in Figures 4 and 5, this is apparently the case. Specifically, the transition function for the ENSO equation is centred approximately around zero, with the two extreme regimes defining strong La Niña and El Niño phases, respectively. Regarding the STVECM for vegetable oil prices, the estimated exponential transition function implies that the transactions cost band is not defined solely by two discrete threshold points, but rather by a continuum of points (locations) connecting the two regimes. The model's dynamics associated with small deviations from long-run equilibrium are defined by the estimated parameters in the first regime, while dynamics associated with the large deviations are defined by incorporating the estimated parameters from both regimes. The observed smooth transition

Table 2 Nonlinearity test results for the system of vegetable price equations

| Transition variable	H_0'''	H_E	H_L	Model
s_{t-1}	5.70E-03	2.30E-01	1.20E-02	LSTVEC
s_{t-2}	3.00E-01	9.40E-01	4.80E-02	
s_{t-3}	1.40E-01	8.40E-01	2.60E-02	
s_{t-4}	1.00E-01	6.10E-01	5.80E-02	
s_{t-5}	6.10E-10	4.70E-06	5.50E-04	ESTVEC
s_{t-6}	5.50E-07	8.30E-06	4.90E-02	ESTVEC
s_{t-7}	**8.60E-07**	**2.00E-07**	**3.30E-01**	**ESTVEC**
s_{t-8}	2.10E-06	1.40E-05	8.60E-02	ESTVEC
s_{t-9}	6.70E-03	7.70E-04	7.30E-01	ESTVEC
s_{t-10}	9.70E-02	4.30E-01	1.10E-01	
s_{t-11}	2.10E-01	1.90E-01	5.80E-01	
s_{t-12}	3.10E-01	1.50E-01	8.10E-01	
F_{RN}	1.4E-05	7.7E-03	2.7E-03	
F_{τ}	9.1E-10	3.6E-04	1.1E-05	
F_{AC}	5.8E-01			

Note: The values in the table represent probability values of the hypotheses being tested; the values in bold represent the selected transition variable and the associated transition function. The tests are performed on autoregressive components of the system, while seasonal components are omitted from the testing framework. The column headed with H_0''' corresponds with the null hypothesis of linearity; the column headed with H_E corresponds with the embedded test against exponential/quadratic nonlinearity, while the column headed with H_L corresponds with the test against logistic nonlinearity; the appropriate models are presented in the column headed with Model. Further, $s_{t-d} = \hat{\bar{e}}_{t-d}$, where $\bar{d} = 1, \ldots, 12$, and where $\hat{\bar{e}}_{t-d}$ is a simple average of the two estimated error correction terms. Finally, F_{RN}, F_{τ} and F_{AC} denote tests against remaining nonlinearity (with respect to the transition variable of choice, i.e. s_{t-3}), parameter nonconstancy and residual autocorrelation, respectively.
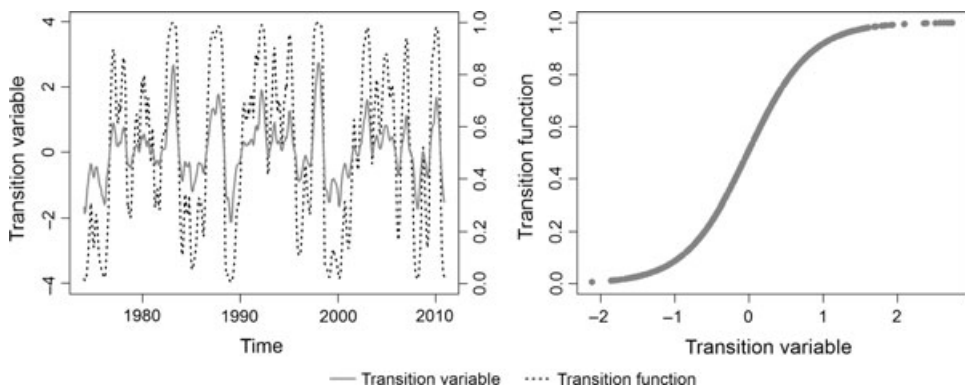
Figure 4 Estimated transition function for the El Niño southern oscillation (ENSO) equation.

between the regimes reveals interesting features of market participants' behaviour in the sense that they are apparently heterogeneous, and perhaps face differing costs for transport, insurance and so forth.

6. ENSO shocks: simulation results

To illustrate the nonlinear effects of ENSO shocks on vegetable oil price dynamics, we adopt the GIRFs approach of Koop *et al.* (1996). GIRFs are
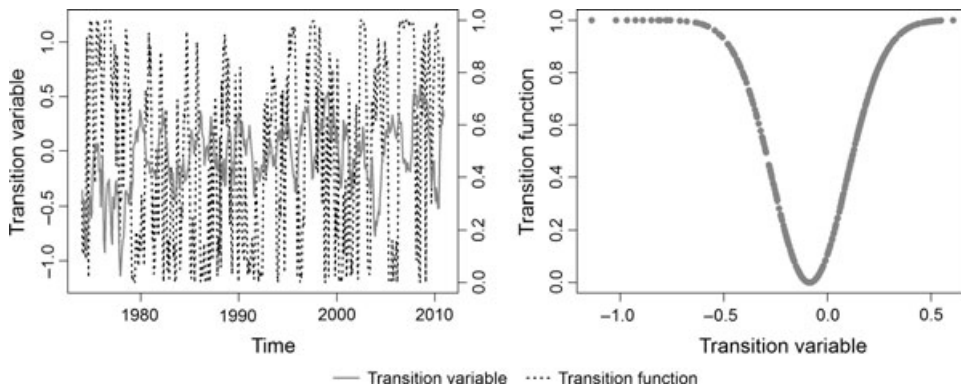
Figure 5 Estimated transition function for the system of price equations.

especially revelatory when analysing the dynamics of nonlinear models, which, unlike linear models, are not invariant to initial conditions—the histories preceding the shocks, the sign and size of the shock, as well idiosyncratic shocks that may occur throughout the forecast horizon. To explore the extent to which there are asymmetries in response to ENSO shocks, and to compare ENSO and vegetable oil price GIRFs for different histories and shocks, we first generate GIRFs by averaging across a subset of initial conditions. Additionally, we select histories corresponding to extreme positive and extreme negative SST anomalies as well as ones that correspond to an effectively neutral regime. These histories are indicated in Figure 3 with vertical lines/stripes. The selected La Niña regime is specified by four consecutive observations (months) beginning with October of 1988 and represents the strongest La Niña episode of the past several decades. The El Niño regime, which we specify by four consecutive observations beginning with October of 1997, represents one of the strongest El Niño episodes in recent history. Finally, from a relatively large number of the candidate histories representing a neutral regime, we select four observations in order to draw comparisons with each of the extreme regimes.

A GIRFs for a particular shock, v, and a subset of histories, $\Im$, is defined as

$$\text{GIRF}(h, v, \Im) = E(y_{t+h}|v, \omega_{t-1} \in \Im) - E(y_{t+h}|\omega_{t-1} \in \Im) \qquad (11)$$

where ω_{t-1} is a particular history (month) within the subset of histories (regime). To numerically evaluate the expected realizations of the GIRFs, we perform 500 bootstrap simulations for each history and shock. The general procedure is outlined in the Technical Appendix (D. Ubilava and M. Holt 2012, unpubl. data, 2012). Under the assumption of strict exogeneity for the ENSO variable, for each iteration we first obtain ENSO forecasts both with and without the initial shock, and by using randomly sampled innovations from the pool of residuals from the estimated ENSO STAR model. In the next stage, the forecasts for the ENSO variable are used to extrapolate

vegetable oil prices from the STVECM, where equation-specific innovations are sampled from the orthogonalised pool of residuals associated with the estimated STVECM. The aforementioned procedure is performed for each selected initial condition and for both positive and negative ENSO shocks. Moreover, we consider shock sizes equal to 1.5 and 3 standard deviations of the estimated ENSO residuals. To obtain a general picture of ENSO effects on vegetable oil prices, we draw 50 histories without replacement, thereby yielding a total of 25,000 GIRF vectors over a 48 month horizon. This process is repeated for each shock sign and size. Additionally, for each history-specific regime, we obtain 2000 bootstrapped vectors of GIRFs, again for each shock sign and size. Mean responses are obtained by averaging the realised GIRFs across the bootstrap iterations and selected histories. Furthermore, the bootstrap resampling procedure allows us to generate an empirical distribution around the expected GIRFs at each point in the forecast horizon.

Following Potter (1995) and van Dijk *et al.* (2002), we use asymmetry measures, ASYs, derived from GIRFs to analyse the nonlinear effects of ENSO shocks on vegetable oil prices. In particular, we are interested in sign-, size- and history-specific asymmetries, which are respectively defined as follows:

$$\text{ASY}_{\pm}(h, v, \omega_{t-1}) = \text{GIRF}(h, v^+, \omega_{t-1}) + \text{GIRF}(h, v^-, \omega_{t-1}) \qquad (12)$$

$$\text{ASY}_v(h, v, \omega_{t-1}) = k\text{GIRF}(h, v, \omega_{t-1}) - \text{GIRF}(h, kv, \omega_{t-1}) \qquad (13)$$

$$\text{ASY}_{\Im}(h, v, \omega_{t-1}) = \text{GIRF}(h, v, \omega_{t-1} \in \Im^+) - \text{GIRF}(h, v, \omega_{t-1} \in \Im^-), \quad (14)$$

where v^+ and v^- are, respectively, positive and negative shocks of the same magnitude; k is a scaler; and finally, $\Im^+$ and $\Im^-$ are subsets of two different regimes from which the histories are selected. It follows, then, that shocks result in symmetric responses if ASYs are symmetrically distributed around zero (van Dijk *et al.* 2002).

First, we consider the expected GIRFs obtained by averaging over 50 histories. These are illustrated in Figure 6, where we also identify 90 per cent confidence intervals of the expected GIRFs. Note that GIRFs associated with negative shocks are multiplied by negative one in order to facilitate comparisons between the shocks of the opposing signs. A number of interesting features are revealed from these graphs. First, ENSO shocks appear to have a statistically significant impact on vegetable oil prices. In particular, a three standard deviation ENSO shock, which corresponds to approximately a 0.7°C SST anomaly, is responsible for about a 6–10 per cent change in vegetable oil prices. As well, El Niño shocks (i.e. a positive shock to the SST anomaly) result in increased prices and La Niña shocks (i.e. a negative shock to the SST anomaly) in decreased prices.
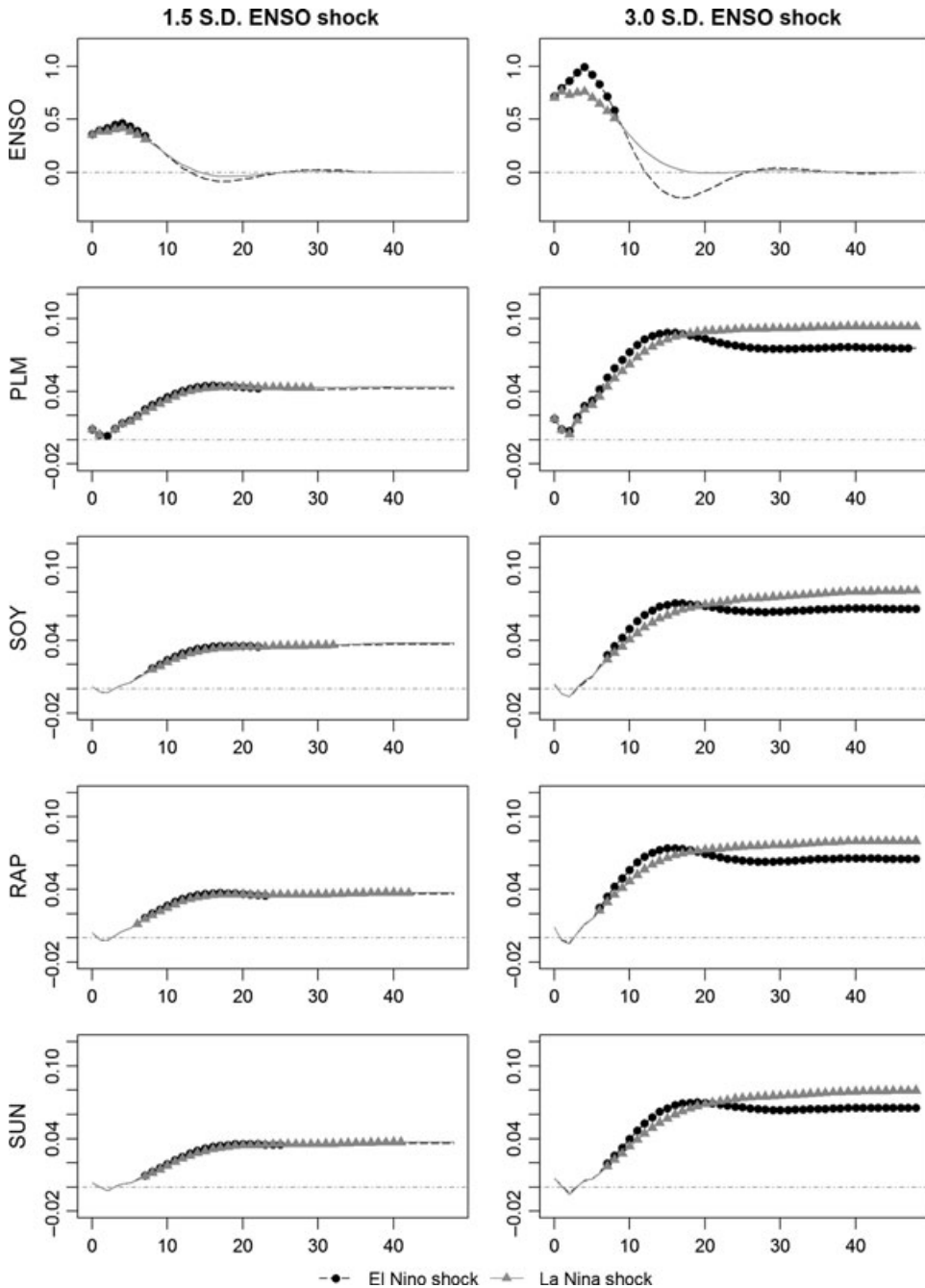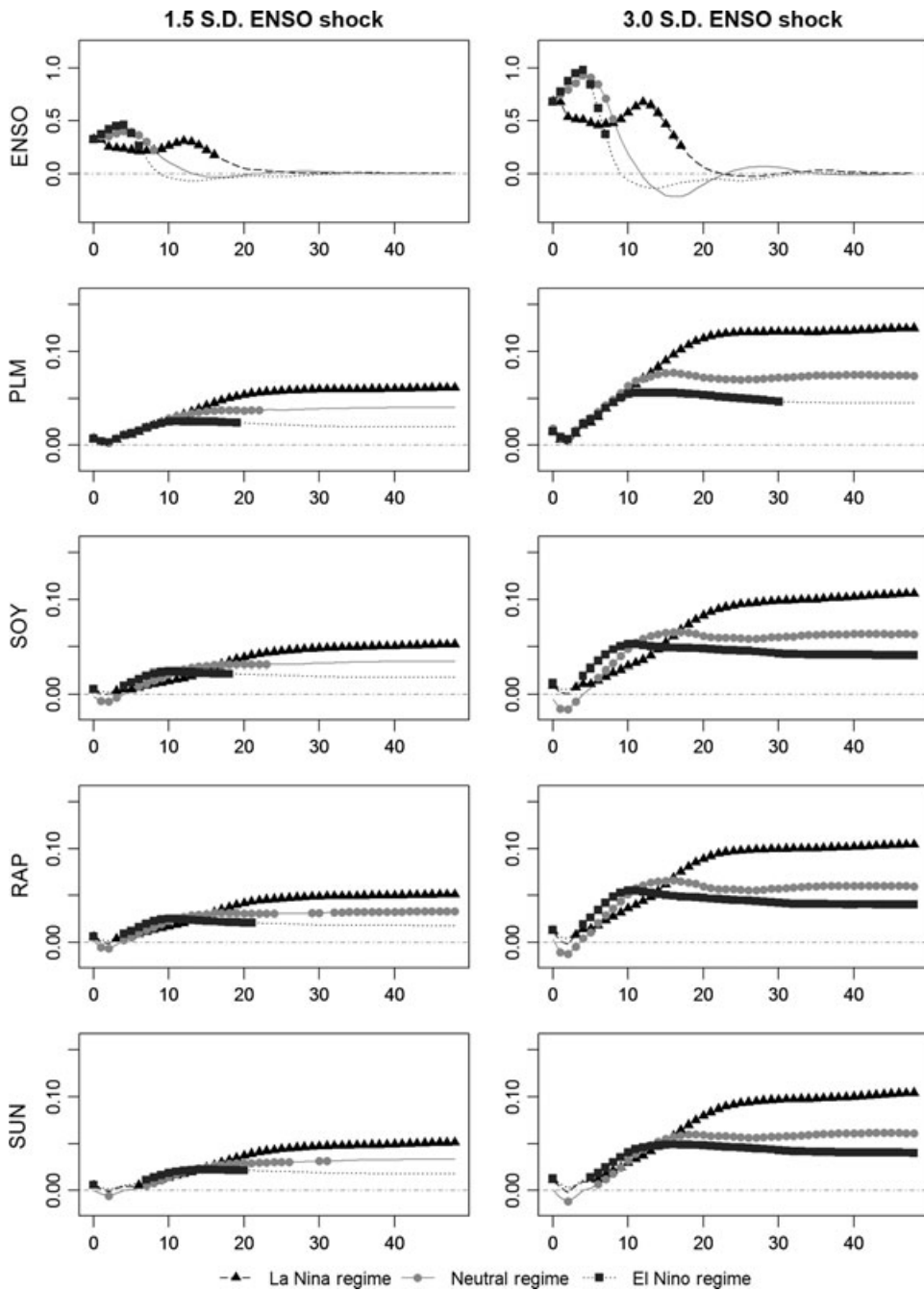
Figure 6 Generalised impulse-response function(GIRFs) of El Nino and La Nina shocks (averaged across 50 histories). Note: Dots denote empirical significance of GIRFs at $\alpha = 0.10$ level; GIRFs associated with negative El Niño southern oscillation (ENSO) shocks are inverted by multiplying realizations by negative one in order to facilitate comparisons between positive and negative shock effects.

Also, of interest are the observed asymmetries in the ENSO as well as the vegetable oil price impulse-response functions. In particular, while the ENSO STAR model implied a mean-reverting process, positive, or El Niño shocks, are more amplified within the first several months as compared with negative, or La Niña shocks. On the other hand, La Niña shocks tend to have a more prolonged effect on ENSO dynamics as compared with El Niño shocks. These results seem to reasonably characterise the ENSO cycle: El Niño phases, while acute, tend to last for shorter periods, often followed with La Niña events, which, in turn, may last for longer periods of time. Additionally, the asymmetries are especially apparent after large ENSO shocks, which also manifest themselves in asymmetric dynamics in vegetable oil prices dynamics. The implication is that a relatively large ENSO shock (either positive or negative) will likely cause a regime switch, resulting in different dynamics as compared to a 'no shock' scenario. In the case of smaller shocks, however, asymmetries are less vivid, partly due to the smooth transition between regimes (both for ENSO and for vegetable oil prices).

To further illuminate the effects of extreme ENSO events, we obtain history-specific GIRFs; see Figure 7. The histories represent extreme ENSO events and are compared to normal conditions, as specified above. Focussing first on the response of the ENSO variable, history-specific asymmetries are readily apparent. While all ENSO GIRFs stabilise by the end of the 3-year horizon, the observed short- and intermediate-term paths vary widely. For example, in the El Niño phase, the shock effects are more amplified in the beginning but also dissipate relatively more quickly as compared with the impulse responses associated with La Niña episodes. Finally, shock signs coupled with initial conditions apparently impact vegetable oil prices differently, thereby inducing ENSO-related asymmetries in price responses as well.

History-specific GIRFs are also used to obtain asymmetry measures, that is, ASYs, as proposed in (12)–(14). As in the case of GIRFs, here too we identify 90 per cent confidence intervals of the expected ASYs with dots of different shape. Sign- and size-specific asymmetries, while on average different from zero, do not reveal statistical significance (figures are available upon request). History-specific asymmetries, however, show statistically significant deviations from zero in the short and intermediate run, wherein the asymmetry measures are derived from the extreme regimes relative to the neutral regime (see Figure 8). The implications are, for example, that a negative (positive) shock during an El Niño (La Niña) event results in a more apparent movement towards La Niña (El Niño) regime than a similar shock that occurs during normal conditions. These effects manifest themselves in history-specific asymmetries of vegetable oil prices as well. For example, in response to the ENSO asymmetries, vegetable oil prices tend to decrease more after ENSO shocks during extreme regimes as compared with a neutral regime.

Figure 7 Generalised impulse-response functions (GIRFs) of El Nino shocks in different El Niño southern oscillation (ENSO) regimes. Note: Dots denote empirical significance of GIRFs at α = 0.10 level.
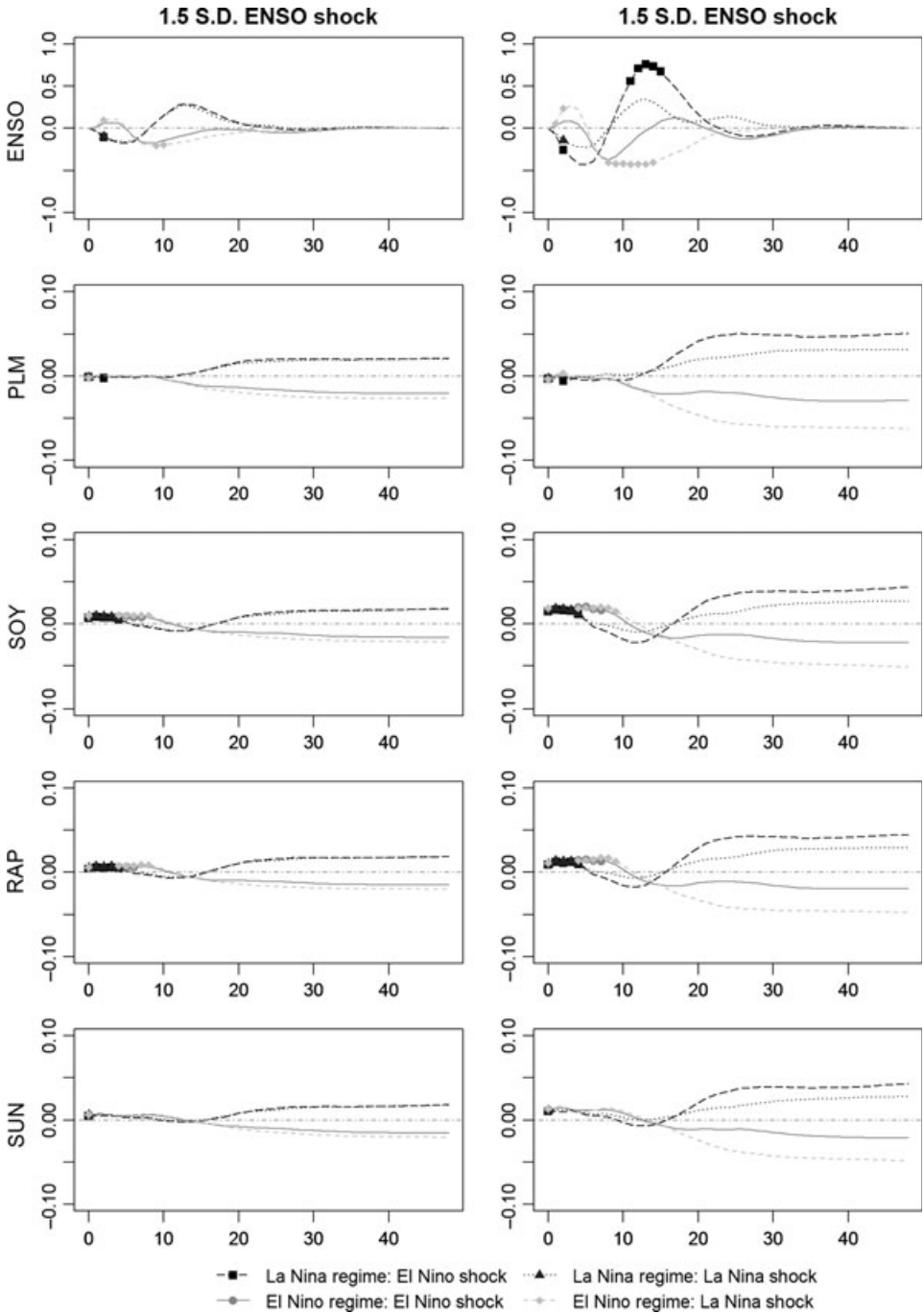
Figure 8 History-specific asymmetries in generalised impulse-response functions of El Niño southern oscillation (ENSO) shocks. Note: Dots denote empirical significance of ASYs at $\alpha = 0.10$ level; ASYs associated with negative shocks are inverted by multiplying realizations by negative one in order to facilitate comparisons between positive and negative shock effects.

Additionally, we assess sign-, size- and history-specific asymmetries by illustrating the empirical distributions of the realised GIRFs at different horizons. In Figure 9, we present Kernel density function estimates of GIRFs at the 12-step-ahead horizon (a more complete set of the distributions are available upon request). These plots further confirm the previously stated findings: there are considerable history-specific asymmetries in ENSO and, to some extent, vegetable oil price dynamics, but there is little evidence for sign- and size-specific asymmetries in the system.

Overall, positive ENSO shocks are followed by increased vegetable oil prices, and the opposite is true for negative ENSO shocks. Therefore, whether or not oilseed producers and consumers are directly affected by an ENSO event, the strong substitutability between these oils results in price co-movements. Negative ENSO shocks tend to have more persistent effects on vegetable oil prices compared to positive ENSO shocks. Again, see Figure 6. This outcome is most likely driven by the relatively prolonged nature of La Niña episodes as compared with the relatively more abrupt nature of El Niño episodes. Interesting patterns are observed across different histories. For example, when initial conditions are in La Niña regime, ENSO shocks (both positive and negative) result in more persistent impulse responses for vegetable oil prices, as compared to the neutral and El Niño regimes.

7. Conclusions

In this paper, we have explored potential nonlinearities in the El Niño–La Niña cycle, and the associated impacts on vegetable oil price dynamics. Consistent with prior research, the results reveal that ENSO dynamics are characterised by self-exciting type nonlinearity. As well, an estimated system of interrelated vegetable oil price equations was found to pose nonlinearity related to the size of the departure from long-run equilibrium relationships. These nonlinearities were further examined by using GIRFs and the derived asymmetry measures. Palm oil, which is largely produced in Oceania and South-East Asia, was found to be significantly impacted by ENSO events. But as importantly, the other vegetable oils, such as soybean oil, sunflowerseed oil and rapeseed oil that are produced in other regions of the world, and regions that are arguably not prone to major climate anomalies resulting from ENSO events, were found to be significantly impacted by ENSO events. This result is perhaps not surprising due to the very strong substitutability in consumption between the oils examined here. Overall, our results reveal that a negative three standard deviation from a normal ENSO regime—that is, a La Niña event—while the corresponding positive results in reduced vegetable oil prices, while the corresponding positive shock—that is, an El Niño event —results in increased vegetable oil prices, and these effects have persistent character.

The results of this research have interesting implications for researchers and policy makers for a number of reasons. First, we model the system of
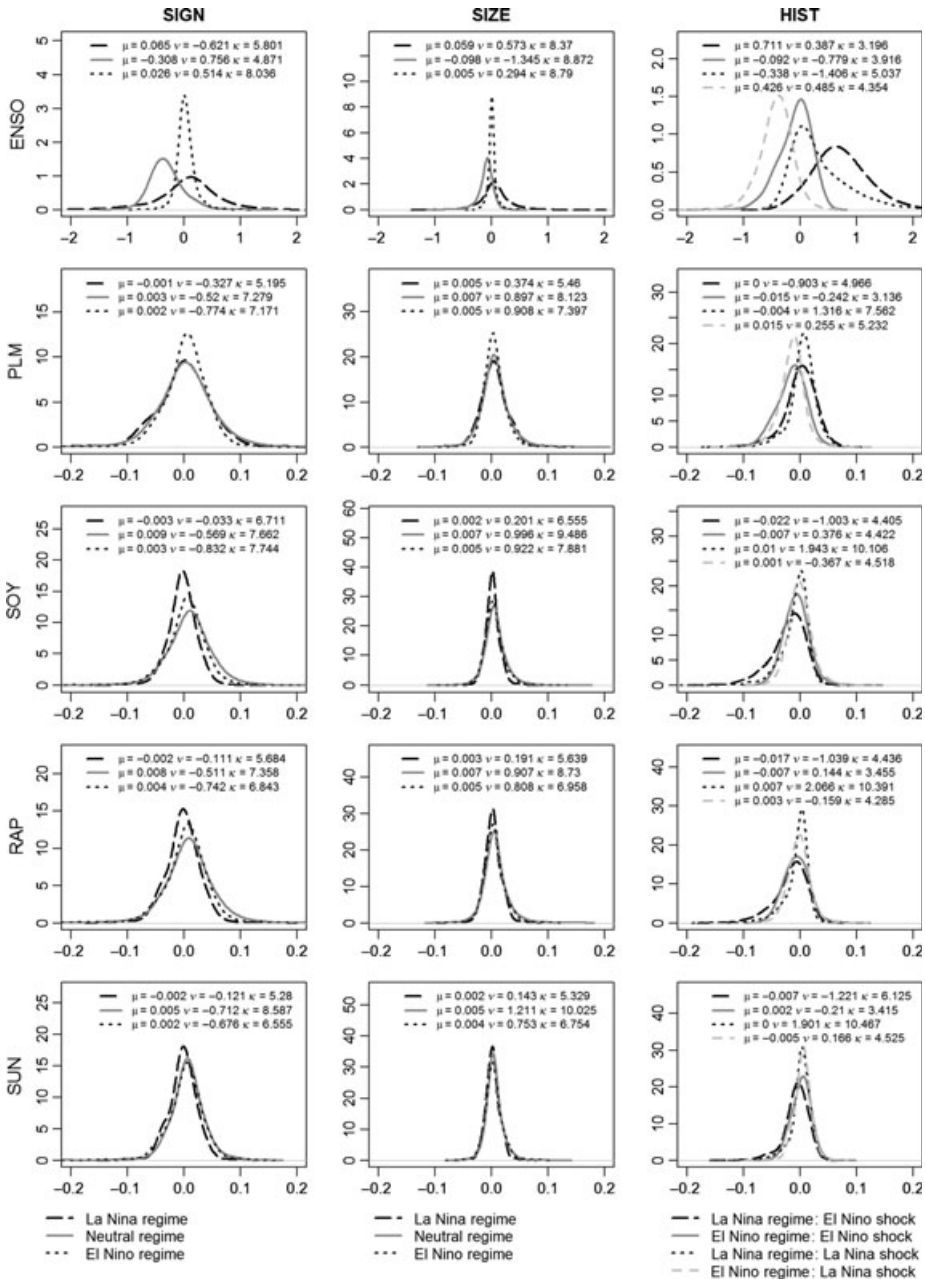
Figure 9 Density distributions of 12-step-ahead generalised impulse-response functions of El Niño southern oscillation (ENSO) shocks. Note: in the case of sign- and history-specific shocks (SIGN and HIST, respectively), the densities are associated with 3 standard deviation ENSO shocks; in the case of size-specific shocks (SIZE), densities are associated with positive ENSO shocks; in the case of HIST, densities associated with negative shocks are inverted by multiplying realizations by negative one in order to facilitate comparisons between positive and negative shock effects; finally, μ denotes mean, v denotes skewness, and κ denotes kurtosis of the associated distributions.

vegetable oil prices using nonlinear time series econometric methods, which improved the overall fit and, potentially, the predictive accuracy of the model. Second, by using ENSO as an explanatory variable in the system, we condition the short- and intermediate-term behaviour of the vegetable oil prices on this exogenous variable—something that has not been done in past, and which allows us to consider, and even predict different scenarios with respect to the state of nature and directions of the ENSO anomaly. Future research should therefore focus on the role of ENSO anomalies for prices of other closely related commodities.

References

Ahti, V. (2009). Forecasting Commodity Prices with Nonlinear Models. Discussion Paper 268, Helsinki Center of Economic Research, University of Helsinki.

An, S.-I. (2009). *A review of interdecadal changes in the nonlinearity of the El Niño – Southern oscillation*, *Theoretical and Applied Climatology* 97(1–2), 29–40.

Balagtas, J.V. and Holt, M.T. (2009). *The commodity terms of trade, unit roots, and nonlinear alternatives: a smooth transition approach*, *American Journal of Agricultural Economics* 91(1), 87–105.

Balke, N. and Fomby, T. (1997). *Threshold cointegration*, *International Economic Review* 38(3), 627–645.

Berry, B.J. and Okulicz-Kozaryn, A. (2008). *Are there ENSO signals in the macroeconomy*? *Ecological Economics* 64(3), 625–633.

Berthelsen, J. (2009). *El Niño is Coming*, *Asia Sentinel*. Available from URL: http://www.asiasentinel.com/index.php, April 8. [accessed 3 April 2010].

Bromokusumo, A.K. and Meylinah S. (2009). El Nino Forecast for Indonesia. GAIN Report ID9036, USDA/FAS, Washington, DC.

Brunner, A. (2002). *El Nino and world primary commodity prices: warm water or hot air? Review of Economics and Statistics* 84(1), 176–183.

Camacho, M. (2004). *Vector amooth transition regression models for U.S. GDP and the composite index of leading indicators*, *Journal of Forecasting* 23(3), 173–196.

Carter, C., Finley, W., Fry, J., Jackson, D. and Willis, L. (2007). *Palm oil markets and future supply*, *European Journal of Lipid Science and Technology* 109(4), 307–314.

Casson, A. (1999). The Hesitant Boom: Indonesia's Oil Palm Sub–Sector in an Era of Economic Crises and Political Change. Centre for International Forestry Research (CIFOR), Bogor, Indonesia.

Davies, R.B. (1977). *Hypothesis testing when a nuisance parameter is present only under the alternative*, *Biometrika* 64(2), 247–254.

Davies, R.B. (1987). *Hypothesis testing when a nuisance parameter is present only under the alternatives*, *Biometrika* 74(1), 33–43.

Debelle, G. and Stevens, G. (1995). Monetary policy goals for inflation in Australia, Research Discussion Paper. 9503. Economic Group, Reserve Bank of Australia.

Demirbas, A. (2008). *Biofuels sources, biofuel policy, biofuel economy and global biofuel projections*, *Energy Conversion and Management* 49(8), 2106–2116.

Enfield, D.B. (2003). The El Niño FAQ: Frequently Asked Questions About El Niño–Southern Oscillation (ENSO). Electronic. Availbale from URL: http://www.aoml.noaa.gov/general/enso_faq/. [accessed 3 April 2010].

Goodwin, B.K., Holt, M.T. and Prestemon, J.P. (2011). *North American oriented strand board markets, arbitrage activity, and market price dynamics: a smooth transition approach*, *American Journal of Agricultural Economics* 93(4), 993–1014.

Hall, A., Skalin, J. and Teräsvirta, T. (2001). *A nonlinear time series model of El Niño*, *Environmental Modelling & Software* 16(2), 139–146.

Hamilton, J.D. (1989). *A New Approach to the Economic Analysis of Nonstationary Time Series and the Business Cycle*, *Econometrica* 57(2), 357–384.

Handler, P. (1984). *Corn yields in the United States and sea surface temperature anomalies in the equatorial Pacific Ocean during the period 1868–1982*, *Agricultural and Forest Meteorology* 31 (1), 25–32.

Handler, P. (1990). *USA corn yields, the El Niño and Agricultural Drought: 1867–1988*, *International Journal of Climatology* 10(8), 819–828.

Handler, P. and Handler, E. (1983). *Climatic anomalies in the tropical Pacific Ocean and corn yields in the United States*, *Science* 220(4602), 1155–1156.

Holt, M.T. and Craig, L.A. (2006). *Nonlinear dynamics and structural change in the U.S. Hog-Corn cycle: a time-varying STAR approach*, *American Journal of Agricultural Economics* 88 (1), 215–233.

In, F. and Inder, B. (1997). *Long-run relationships between world vegetable oil prices*, *The Australian Journal of Agricultural and Resource Economics* 41(4), 455–470.

Ismail, M.T. (2011). Modelling nonlinear relationship among vegetable oil price time series, In ICMSAO 2011: Fourth International Conference on Modeling, Simulation and Applied Optimization, pp. 1–5.

Jansen, E.S. and Teräsvirta, T. (1996). *Testing parameter constancy and super exogeneity in econometric equations*, *Oxford Bulletin of Economics and Statistics* 58(4), 735–763.

Keppenne, C. (1995). *An ENSO signal in soybean futures prices*, *Journal of Climate* 8(6), 1685–1689.

Ker, A.P. and McGowan, P. (2000). *Weather-based adverse selection and the U.S. Crop Insurance Program: the private insurance company perspective*, *Journal of Agricultural and Resource Economics* 25(2), 386–410.

Koop, G., Pesaran, M. and Potter, S. (1996). *Impulse response analysis in nonlinear multivariate models*, *Journal of Econometrics* 74(1), 119–147.

Kuan, C.-M. and White, H. (1994). *Artificial neural networks: an econometric perspective*, *Econometric Reviews* 13(1), 1–91.

Labys, W. (1977). *Multicommodity substitution patterns in the international fats and oils market*, *European Review of Agricultural Economics* 4(1), 75–84.

Lamb, H. (1995). Climate, History, and the Modern World, 2nd edn. Routledge, London and New York.

Letson, D. and McCullough, B. (2001). *ENSO and soybean prices: correlation without causality*, *Journal of Agricultural and Applied Economics* 33(3), 513–522.

Lin, C.-F.J. and Teräsvirta, T. (1994). *Testing the constancy of regression parameters against continuous structural change*, *Journal of Econometrics* 62(2), 211–228.

Luukkonen, R., Saikkonen, P. and Teräsvirta, T. (1988). *Testing Linearity Against Smooth Transition Autoregressive Models*, *Biometrika* 75(3), 491–499.

Milas, C. and Legrenzi, G. (2006). *Non-linear real exchange rate effects in the UK labour market*, *Studies in Nonlinear Dynamics & Econometrics* 10(1), 1285–1285.

Milas, C. and Rothman, P. (2008). *Out-of-sample forecasting of unemployment rates with pooled STVECM forecasts*, *International Journal of Forecasting* 24(1), 101–121.

Owen, A.D., Chowdhury, K. and Garrido, J.R.R. (1997). *Price interrelationships in the vegetable and tropical oils market*, *Applied Economics* 29(1), 119–124.

Potter, S. (1995). *A nonlinear approach to U.S. GNP*, *Journal of Applied Econometrics* 10(2), 109–125.

PSD Online (2011). USDA Foreign Agricultural Service. Available from URL: http://www.fas.usda.gov/psdonline. [accessed 11 December 2011].

Rothman, P., van Dijk, D. and Franses, P.H. (2001). *Multivariate STAR analysis of money–output relationship*, *Macroeconomic Dynamics* 5, 506–532.

Schlenker, W. and Roberts, M. (2006). *Nonlinear effects of weather on corn yields*, *Review of Agricultural Economics* 28, 391–398.

Schlenker, W. and Roberts, M.J. (2009). *Nonlinear temperature effects indicate severe damages to U.S. crop yields under climate change*, *Proceedings of the National Academy of Sciences* 106 (37), 15594–15598.

Schmidt, J. and Weidema, B. (2008). *Shift in the marginal supply of vegetable oil*, *The International Journal of Life Cycle Assessment* 13(3), 235–239.

Shahwan, T. and Odening, M. (2007). Forecasting agricultural commodity prices using hybrid neural networks, in Chen, S.-H., Wang, P.P. and Kuo, T.-W. (eds.), Computational Intelligence in Economics and Finance, Vol. II. Springer, Berlin and Heidelberg, pp. 63–74.

Temin, P. (2002). *Price behavior in ancient Babylon*, *Explorations in Economic History* 39, 46–60.

Teräsvirta, T. (1994). *Specification, estimation, and evaluation of smooth transition autoregressive models*, *Journal of the American Statistical Association* 89(425), 208–218.

Tong, H. (1990). Non-Linear Time Series: A Dynamical System Approach. Oxford University Press, Oxford, UK.

Tsay, R. (1989). *Testing and modeling threshold autoregressive processes*, *Journal of the American Statistical Association* 84(405), 231–240.

Ubilava, D. (2012). *Modeling nonlinearities in the U.S. soybean-to-corn price ratio: a smooth transition autoregression approach*, *Agribusiness* 28(1), 29–41.

van Dijk, D., Franses, P. and Paap, R. (2002). *A nonlinear long memory model, with an application to U.S. unemployment*, *Journal of Econometrics* 110(2), 135–165.

Walker, G. (1923). *Correlation in seasonal variations of weather. VIII. A preliminary study of world–weather*, *Memoirs of the Indian Meteorological Department* 24(4), 75–131.

Supporting Information

Additional Supporting Information may be found in the online version of this article:

Data S1. The modelling Framework.

Figure S1. Representative LSTAR, QSTAR and ESTAR transition functions.

Table S1. Augmented Dickey–Fuller test statistics.

Table S2. Johansen cointegration test results.

Table S3. Nonlinearity test results for the ENSO equation.

Table S4. Nonlinearity test results for the system of equation.